Optical Carrier-Suppressed Single Sideband (O-CS-SSB) Modulation Using a Hyperfine Blocking Filter Based on a Virtually Imaged Phased-Array (VIPA)

Shijun Xiao, *Student Member, IEEE,* and Andrew M. Weiner, *Fellow, IEEE*

***Abstract*—Using a hyperfine blocking filter based on a virtually imaged phased-array as the spectral disperser, we present a novel scheme of optical carrier-suppressed single sideband (SSB) modulation. Our experiments demonstrate sideband suppression of ∼28 dB at only a 2.9-GHz offset for single subcarrier amplitude modulated at 622 Mb/s. Furthermore, the hyperfine blocking filter can be tuned for simultaneous optical SSB and strong carrier suppression to ∼30 dB lower in optical power than the unsuppressed sideband.**

***Index Terms*—Microwave photonics, single sideband (SSB) modulation, subcarrier multiplexing (SCM), virtually imaged phased-array (VIPA).**

SUBCARRIER multiplexing (SCM) is a relatively new scheme in high-speed radio-fiber links [1], [2]. This technique gains advantages by the use of mature microwave signal processing techniques since microwave devices have several advantages over optical devices: the stability of oscillators, the frequency selectivity of filters, and the ease of implementing advanced modulation formats. In order to reduce power fading caused by fiber dispersion and increase spectral efficiency, optical single sideband (O-SSB) modulation is widely used in SCM. Optical carrier suppression is also important in order to improve modulation depths and thereby increase receiver sensitivity. Previous optical carrier-suppressed single sideband (O-CS-SSB) modulation experiments used relatively complex electronics and obtained sideband suppression limited to 15 dB (due to modulator nonlinearity) [1], [2]. Carrier suppression was obtained either via an optical Fabry–Pérot notch filter that must be precisely matched to the carrier frequency [1] or via tuning the modulator bias (in which case the carrier remained 8 dB higher than the unsuppressed sideband, again limited by modulator nonlinearity) [2]. Another O-CS-SSB modulation experiment reported in [3] has a similar design compared to that in [2], but the carrier suppression is dependent on very precise fiber coupler ratios and radio-frequency driving voltages. Recently, O-SSB modulation based on optical fiber Bragg grating (FBG) filtering in a tandem structure [4] was demonstrated with high sideband suppression (>20 dB). This experiment was limited to subcarriers with >7-GHz frequency offset due to FBGs spectral resolution; neither data modulation nor carrier suppression were reported.

Manuscript received Febuary 22, 2005; revised March 21, 2005. This work was supported in part by the ARO under Grant DAAD19-03-1-0275.

The authors are with the School of Electrical and Computer Engineering, Purdue University, West Lafayette, IN 47907-2035 USA (e-mail: sxiao@ecn.purdue.edu; amw@ecn.purdue.edu).

Digital Object Identifier 10.1109/LPT.2005.848564

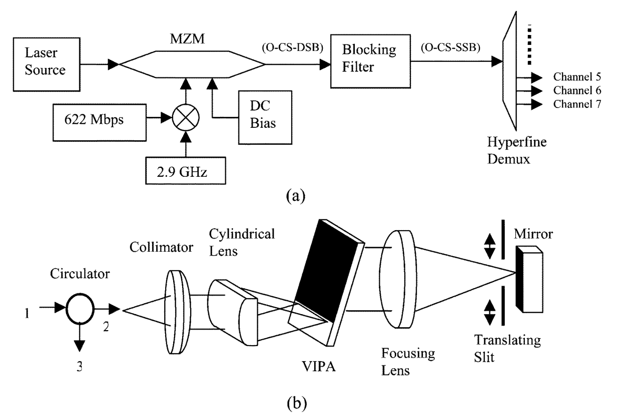

Fig. 1. (a) Setup for O-CS-SSB modulation; (b) setup for the hyperfine blocking filter.

O-SSB with strong carrier suppression has been the most efficient modulation format in radio-fiber links since the only power transmitted is the information sideband [5], [6]. Therefore, achieving simultaneous high sideband suppression and greater carrier suppression may allow increased dynamic range and spectral efficiency. In this letter, we introduce a hyperfine blocking filter for O-CS-SSB modulation, which allows us to demonstrate sideband suppression of ∼28 dB at only 2.9-GHz offset. Furthermore, the blocking filter can be tuned for simultaneous SSB and strong carrier suppression (down to ∼30 dB lower than the unsuppressed sideband). As a result, we demonstrate here, for the first time to our knowledge, simultaneous frequency translation (by 2.9 GHz) and data encoding and detection (622 Mb/s), which brings new prospects for high spectral efficiency in microwave photonics.

Fig. 1(a) shows our experimental setup. We use a tunable laser source (Agilent 81 680 A) with an output wavelength at 1.55 μm and a spectral linewidth below 0.1 pm (12.5 MHz) for the input (6 dBm in power) to a standard single electrode-drive Mach–Zehnder modulator (MZM) with an electrical 3-dB passband ∼30 GHz and a null transmission bias voltage $V_\pi =$ 4.5 V. The MZM is modulated by the output of a microwave mixer mixing a subcarrier at 2.9 GHz and a 622-Mb/s pseudo-random binary sequence in amplitude shift keying. The MZM's

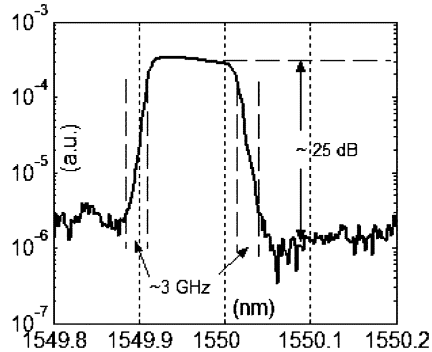

Fig. 2. One example of the tunable blocking filter's transmission spectrum over one FSR.

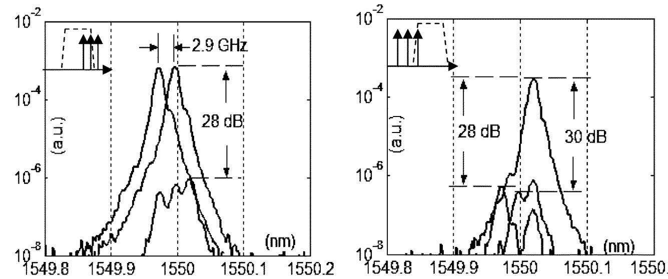

(a) (b)

Fig. 3. (a) Superimposed output spectra from the hyperfine demux for O-CS-SSB modulation with partial carrier suppression. (b) Superimposed output spectra from the hyperfine demux for O-CS-SSB with high carrier suppression, blocking both the upper frequency sideband and the carrier. The insets sketche the position of the blocking filter.

output spectrum has three spectra peaks corresponding to a partial suppressed optical carrier and double sidebands spaced at ±2.9 GHz from the carrier (optical carrier-suppressed double sideband) [6]. The MZM's total optical insertion loss is ~20 dB including an intrinsic loss ~6 dB, with the remaining loss due to bias near the minimum transmission point. After being amplified through an erbium-doped fiber amplifier to a power level ~0 dBm, the MZM's output goes through a hyperfine blocking filter based on a relatively new optical disperser termed as virtually imaged phased-array (VIPA). One important application of the VIPA is in dispersion compensation [8], [9] in a reflective geometry. Here, we demonstrate another new application of the VIPA as a hyperfine blocking filter, again in the reflective geometry. Fig. 1(b) shows the setup of our hyperfine blocking filter based on a solid VIPA with a 50-GHz free-spectral range (FSR). The setup is similar to that used in the VIPA dispersion compensators except that we use a ~100% reflective flat mirror instead of a curved mirror. In theory, this setup can be free of dispersion [8], [9]. In addition, we use a slit placed close to the mirror plane, which can be translated laterally to shift the passband of the filter. The filter can be adjusted to block either one sideband only or both one sideband and the carrier. The slit can also be opened up to pass the entire spectrum for diagnostic purposes. The average total insertion loss is ~13 dB, which is in the same range reported in [8] and [9]. With a perfect implementation, the insertion loss can be theoretically reduced to about 5 dB [8]. Fig. 2 shows one filtering example, zoomed in to view a single FSR; this is the setting used in our following measurements in Fig. 3(a). The transition of the filter from OFF to ON state occurs in ~3 GHz, for a transmission change of ~25 dB. This indicates a rolloff of the transmittance function of ~1000 dB/nm, which is five times higher than that (200 dB/nm) reported in [4] using two FBGs in series. As our optical spectrum analyzer (OSA) has a resolution limited to 10 pm (1.25 GHz), we use three channels (channel spacing matched to 2.9 GHz) from an eight-channel hyperfine wavelength demultiplexer based on a second solid VIPA [10] to separate the optical carrier and the two sidebands. The wavelength demultiplexer has an insertion loss 12.5 dB for each of the three channels. The three spatially separated outputs are then detected on at a time by the OSA. By superimposing the OSA measurements for each of the three channels into a single plot, we can characterize the sideband or carrier suppression performance of our apparatus.

One application of the blocking filter is in suppressing one sideband after direct double sideband modulation. The blocking filter is positioned to suppress the lower frequency (longer wavelength) sideband [see inset to Fig. 3(a)]; the carrier is suppressed independently by tuning the MZMs bias. Fig. 3(a) shows superimposed output spectra after the hyperfine demultiplexer for O-CS-SSB modulation with partial carrier suppression (MZM biased at 4.2 V). The suppressed lower frequency sideband is ~28 dB lower in peak power than the unsuppressed upper frequency sideband. The sideband suppression is improved by over 10 dB compared to previous results in [1] and [2]. The carrier and remaining sideband have approximately equal power, which would be near optimum for detection by heterodyne beating as in conventional SCM links. Note that it is very easy to increase the carrier power in our experiments by tuning the bias voltage applied to the MZM while maintaining stable sideband suppression, since the sideband suppression is controlled by the blocking filter independently. This would be useful for SCM links with multiple subcarriers since the carrier must be higher than the combined maximum magnitude of all subcarriers for heterodyne detection [1], [2]. Another application of the blocking filter is for simultaneous sideband suppression and carrier suppression. Fig. 3(b) shows superimposed output spectra for O-CS-SSB modulation with strong carrier suppression, with the MZM biased at the minimum transmission point $(V = V_\pi)$. Please note that in these experiments the filter passband is different compared to that used in Fig. 3(a). Without the blocking filtering, there is a residual carrier (5 dB lower in peak power than the sideband in our case) attributed to the chirp that occurs for modulation with single electrode-drive and to modulator nonlinearity, which limit carrier suppression. Using our hyperfine blocking filter, we can break these limits and easily obtain a tunable stronger carrier suppression. Fig. 3(b) shows an example of O-CS-SSB modulation with very high carrier suppression: The carrier is 30 dB lower in peak power than the unsuppressed lower frequency sideband, and upper sideband suppression is maintained at ~28 dB. Here, the filter is positioned to block both the upper sideband and the carrier [Fig. 3(b)].

A good test of SSB generation with high carrier suppression is provided by the eye diagrams. For high-quality O-CS-SSB, the eye should be wide open in direct detection. For incomplete carrier suppression, however, coherent interference between the residual carrier and the SSB leads to eye closure (this is in contrast to conventional SCM links with heterodyne detection, where no eye opening is observed until the heterodyne signal

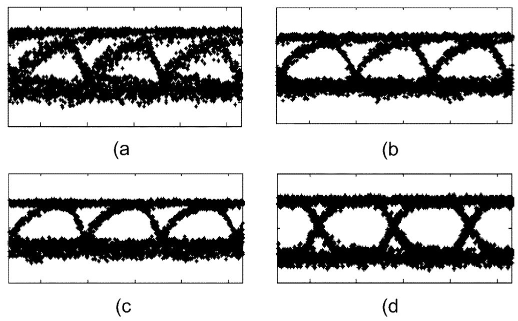

Fig. 4. Typical eye diagrams for O-CS-SSB with carrier suppression ratios of (a) 5, (b) 10, (c) ≥15 dB below the remaining sideband, and (d) for direct intensity modulation without subcarrier or blocking filter. The sideband suppression is maintained at 28 dB.

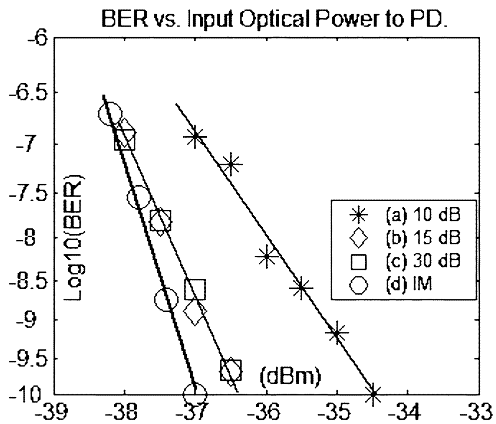

Fig. 5. BER for O-CS-SSB with carrier suppression ratios of (a) 10, (b) 15, (c) 30 dB below the remaining sideband, and (d) for direct intensity modulation without subcarrier or blocking filter. The sideband suppression is maintained at 28 dB.

is mixed with a microwave oscillator). In our tests, eye diagrams are measured directly at the blocking filter output. The eight-channel hyperfine wavelength demultiplexer is not used. The filter output is detected using a receiver with 3-dB electrical bandwidth of ~0.5 GHz for 622-Mb/s ON–OFF keying (OC-12). Fig. 4(a)–(c) shows typical eye diagrams for carrier suppression ratios of (a) 5, (b) 10, and (c) ≥15 dB below the remaining sideband, respectively. In each case, the suppressed sideband is down by ~28 dB. For reference, Fig. 5(d) shows the eye diagram measured directly at the output of the MZM with external intensity modulation (no subcarrier, no blocking filter). The optical power to the photodiode is approximately the same for all eye diagram measurements. Fig. 4(a) indicates a seriously closed eye for carrier suppression to 5 dB below the unsuppressed sideband. The eye diagrams open up with increased carrier suppression, and reach maximum opening for carrier suppression ratios ≥15 dB lower than the remaining sideband. However, there is still distortion compared to direct external intensity modulation [Fig. 4(d)]. These effects are further confirmed by the bit-error-rate (BER) test. Fig. 5 shows the BERs for carrier suppression ratios of 10, 15, and 30 dB (relative to the remaining sideband) as well as the BER at the output of MZM with direct intensity modulation (no subcarrier) for comparison. Our results indicate that the BER depends sensitively on the suppression ratio. Compared to direct intensity modulation, carrier suppression ratios relative to the remaining sideband of less than 10 dB result in a large power penalty (≥2.5 dB). Carrier suppression ratios of 15 and 30 dB result in a power penalty ~0.5 dB; carrier suppression in excess of 15 dB below the remaining sideband does not lead to further reduction in the power penalty. The 0.5-dB power penalty may be caused by effects from the blocking filtering (slight sideband shaping and slight chromatic dispersion) as well as amplified spontaneous emission noise from the EDFA.

In summary, we have introduced a hyperfine blocking filter for O-CS-SSB modulation, and we demonstrate sideband suppression of ~28 dB at only 2.9-GHz offset. Furthermore, the blocking filter can be tuned for simultaneous SSB and strong carrier suppression (to 30 dB below the unsuppressed SSB). As a result, we demonstrate data encoding and detection at 622 Mb/s with simultaneous 2.9-GHz frequency translation. Our scheme as currently demonstrated should be applicable for O-CS-SSB modulation for multiple subcarriers with carrier frequencies spanning from ~3 to ~25 GHz. Our scheme should also be applicable to phase modulation for coherent SCM links.

ACKNOWLEDGMENT

The authors would like to thank C. Lin from the Avanex Corporation for providing the VIPA samples and Prof. D. Seo for discussion and help.

REFERENCES

[1] R. Hui, B. Zhu, R. Huang, C. T. Allen, K. R. Demarest, and D. Richards, "Subcarrier multiplexing for high-speed optical transmission," *J. Lightw. Technol.*, vol. 20, no. 3, pp. 417–427, Mar. 2002.

[2] A. Loayssa, C. Lim, A. Nirmalathas, and D. Benito, "Optical single-sideband modulator for broad-band subcarrier multiplexing systems," *IEEE Photon. Technol. Lett.*, vol. 15, no. 2, pp. 311–313, Feb. 2003.

[3] M. Y. Frankel and R. D. Esman, "Optical single-sideband suppressed-carrier modulator for wide-band signal processing," *J. Lightw. Technol.*, vol. 16, no. 5, pp. 859–863, May 1998.

[4] J. Capmany, B. Ortega, A. Martinez, D. Pastor, M. Popov, and P. Y. Fonjallaz, "Multiwavelength single sideband modulation for WDM radio-over-fiber systems using a fiber grating array tandem device," *IEEE Photon. Technol. Lett.*, vol. 17, no. 2, pp. 471–473, Feb. 2005.

[5] G. E. Betts, "High dynamic range coherent analog links using AM-SSB," in *LEOS Ann. Meeting*, Puerto Rico, Nov. 2004, Invited paper MN3.

[6] R. Montgomery and R. DeSalvo, "Novel technique for double sideband suppressed carrier modulation of optical fields," *IEEE Photon. Technol. Lett.*, vol. 7, no. 4, pp. 435–437, Apr. 1995.

[7] M. Shirasaki, "Large angular dispersion by a virtually imaged phased array and its application to a wavelength demultiplexer," *Opt. Lett.*, vol. 21, pp. 366–368, 1996.

[8] ——, "Chromatic-dispersion compensator using virtually imaged phased array," *IEEE Photon. Technol. Lett.*, vol. 9, no. 12, pp. 1598–1561, Dec. 1997.

[9] ——, "Compensation of chromatic dispersion and dispersion slope using a virtually imaged phased array," in *Opt. Fiber Commun. Conf.*, Anaheim, CA, Mar. 18–23, 2001, Paper TuS1.

[10] S. Xiao and A. M. Weiner, "An eight-channel hyperfine wavelength demultiplexer using a virtually imaged phased-array (VIPA)," in *IEEE Photon. Technol. Lett.*, vol. 17, Feb. 2005, pp. 372–374.